

**STRUCTURAL AND OPTICAL PROPERTIES OF ELECTROCHEMICALLY  
FABRICATED TiO<sub>2</sub> THIN FILMS****Sh.O. EMINOV, Kh.D. JALILOVA, S.A. ALIYEV, N.N. MUSAYEVA, A.A. RAJABLI,  
G.H. MAMMADOVA, J.A. GULIYEV, S.H. ABDULLAYEVA, I.I. GURBANOV***Institute of Physics of NAS Azerbaijan, H.Javid ave., 131, AZ1143, Baku, Azerbaijan**e-mail : shikhamirem@gmail.com*

Several key aspects of the self-organization of nanotubes in RF sputtered titanium (Ti) thin films formed by the anodization process has been investigated. Fabrication procedures included radiofrequency magnetron deposition of InSnO<sub>2</sub> (*ITO*) thin film and Ti thin films on transparent glass wafer followed with electrochemical anodization of Ti in fluorine and aqueous-containing electrolytes. Finally, the obtained Glass/*ITO*/TiO<sub>2</sub> structures were annealed at 450°C for 2h in the air to convert the amorphous both as-anodized TiO<sub>2</sub> and *ITO* into crystalline ones. The observation of surface morphology for TiO<sub>2</sub> films carried out using both atomic force microscopy operating in contact mode and by scanning electron microscope. The structural properties of the samples were characterized by using X-ray diffractometry. The optical properties were studied by using spectroscopic ellipsometry, *UV-VIS* spectrophotometry, as well as Raman spectroscopy. Highly ordered *TNT* arrays of 40-45nm pore diameter with a high degree of optical transmission were obtained. It has been established that, anodization time has an effect on the surface morphology and regularity of the pores. The longer the anodization time, the more regular are the porous structure. *XRD* pattern of the TiO<sub>2</sub> /*ITO* structure has shown the existence of the anatase phase of polycrystalline TiO<sub>2</sub>. Polyform phases of rutile and brookite weren't revealed. The films are transparent in the region of 900-360nm with a transmittance of about 70–80% of light and exhibit strong absorption in the *UV* region with a wavelength shorter than 360nm. The Raman spectra confirm the presence of most of the modes directly typical only of the anatase phase and exclude the presence of rutile and brookite phases. Ellipsometry studies allowed it to create an optical model of experimentally obtained glass/*ITO*/TiO<sub>2</sub> structure consisting of five layers with different thicknesses and constituents.

**Keywords:** *TNT*, TiO<sub>2</sub>; InSnO<sub>2</sub>, *ITO*, magnetron sputtering, anodic oxidation, TiO<sub>2</sub> nanotube**PACS:** 78.67. Rb, 78.67. Qa, 78.67. Bf, 81.07. De, 88.40. H**1. INTRODUCTION**

The development of metal oxide thin films of controlled surface roughness and complexity presents a significant theoretical and technological importance, offering an exciting opportunity for developing a new class of materials with unique physical, chemical, optical and electronic properties [1-7]. Owing to their advanced physical and chemical properties and potential applications in the field of solar energy collection, bio nano- and gas sensors, catalysts, etc., a self-organized, highly ordered array of cylindrical shaped titanium dioxide (TiO<sub>2</sub> or titania) thin films have recently attracted a particularly increased attention because of their extended use in a multitude of applications.

This material is a non-toxic and biocompatible wide-bandgap (3.2–3.30eV) *n*-type semiconductor with extremely high resistivity. It can exist in three main polymorphs: namely anatase, rutile, and brookite.

The first two of them exhibit a tetragonal crystal structure, whereas the third of them (brookite) has an orthorhombic crystal structure. TiO<sub>2</sub> is one of the most desired photocatalysts for environmental and renewable energy applications.

Nanotube arrays of TiO<sub>2</sub> (*TNT*) have many excellent properties such as specific surface area, high adsorption capacity, and so on. They are being applied to many fields, such as environmental applications including the purification of wastewater, hydrogen generation by water splitting, solar photovoltaic based electricity production, gas sensor, and so on [1-12]. In

[12] it has been stated that this better catalytic activity of TiO<sub>2</sub>/*ITO* samples is related to a perfect crystalline structure, preventing the recombination of charge carriers.

Because TiO<sub>2</sub> films have a high refractive index and demonstrate high photocatalytic activity, they are usually placed directly onto the top of transparent conductive indium tin oxide (*ITO*) films [14,15]. The ability to control the properties of *TNT* layers formed on transparent and conductive substrates is the key to practical applications in various fields.

Many techniques have been used to prepare TiO<sub>2</sub> films [8-12], such as reactive magnetron sputtering chemical vapor deposition, pulsed laser deposition, sol-gel deposition), and reactive sputtering and anodic oxidation.

The anodic oxidation technique has emerged as one of the most promising techniques. Since the first decades of the 20th century, this electrochemical process has been intensively used for a broad range of industrial applications, including surface finishing, automobile engineering, machinery, corrosion protection, and so on.

The use of electron microscopes in the 1950s revealed the nanoporous and nanotubular structure of anodic oxides and made it possible to establish the effect of the different fabrication parameters on the physical and chemical properties of the prepared structures.

In this work, we present the results of investigations on processing and nanostructural characteristics of TiO<sub>2</sub> porous thin films grown on the transparent glass substrates using magnetron sputtering

techniques, electrochemical anodization, as well as thermal annealing.

## 2. EXPERIMENTAL

### 2.1. Preparation of Glass/ITO/TiO<sub>2</sub> structure

The glass substrates were cut into 1.5 by 2 cm pieces and then ultrasonically cleaned in acetone and methanol, rinsed in double-distilled water sequentially, and blow-dried with a nitrogen gun. Afterward, the glass substrates were loaded into the deposition chamber of the Leybold Heraeus-Z550 RF magnetron sputtering system. Then, ITO films with thicknesses varying from 80 to 400 nm were sputtered on them at room temperature in a mixed Argon /O<sub>2</sub> gases mixture using an ITO target (In<sub>2</sub>O<sub>3</sub>/SnO<sub>2</sub>, 90/10 wt.%) [14]. Thereafter, the Titanium layer with a thickness in the range of 150 to 200 nm was sputtered on previously obtained glass/ITO substrates in the same chamber using the titan target. Then, TiO<sub>2</sub> thin film was formed by electrochemical anodization of as-grown Ti film in a homemade two-electrode cell using a Pt mesh as a counter electrode and Ti/ITO/glass substrate as anode under a constant potential ranging from 10 to 60V at 3–5°C. The mixture of ethylene glycol, 0.4wt % ammonium fluoride, and 2 vol.% distilled water was used as an electrolyte. The duration of anodization ranged from a few minutes to several tens of minutes, depending upon the thickness of the Ti layer. To maintain the set temperature during the anodization process, the electrochemical cell was kept in a container with icy water. The samples were removed from the electrolyte after they became optically transparent, and the value of the anodization current dropped to zero. The anodized samples were washed in isopropyl alcohol and distilled water for about 5 min and blow-dried with nitrogen. The obtained glass/ITO/TiO<sub>2</sub> structures finally were annealed for 2 h in the air at 450°C to improve the crystallinity and electrical

characteristics of both external TiO<sub>2</sub> and the internal ITO thin film.

### 2.2. Characterization Techniques

Supra TM35vp Scanner electron microscope, as well as AFM, was used to investigate the surface morphology of the samples. X-ray diffraction patterns were obtained using an X-Ray D2Phaser (Bruker) diffractometer (Cu-Kα ( $\lambda=1.54021\text{Å}$ )). The UV-Vis optical transmittance spectrum was recorded by using a Specord-210 spectrophotometer in the range 300–900nm. A Nanofinder 30-NM01 Confocal Raman microscope with an excitation 633nm laser was used to study the vibrational properties of the samples. To study the microstructure characteristics of the films, the J.A. Woollam-M2000 (USA) spectroscopic ellipsometer was used for variable angle spectroscopic ellipsometry (VASE) measurements at room temperature in the photon energy range 0.73–4.0eV at an incident angle of 75°.

## 3. RESULTS AND DISCUSSION

### 3.1 Structural properties

Figure 1 shows the XRD pattern of glass/ITO/TiO<sub>2</sub> thin film. The diffractogram shows reflections of the anatase TiO<sub>2</sub> with a predominant (101) peak (at  $2\theta=25.5^\circ$ ) and cubic In<sub>2</sub>O<sub>3</sub> ITO thin film. It can be seen that the pattern seems to be anatase. In fact, under these specific preparation conditions, the films are comprised of single anatase. The presence of the anatase polyform phase of TiO<sub>2</sub> with a tetragonal structure ( $a=3.799\text{Å}$ ,  $c=9.509\text{Å}$ ;  $Z=4$ ) is confirmed by strong diffraction peaks at  $2\theta=25.5, 37^\circ, 48^\circ, 54.1^\circ, 62.5^\circ$  and  $67^\circ$ . These peaks appear as reflections from (101), (004), (200), (105), (204) and (116) planes of anatase, respectively, and match well with the JCPDS file no PDF 03-065-5714. No trace of rutile and brookite phases was detected in the XRD pattern.

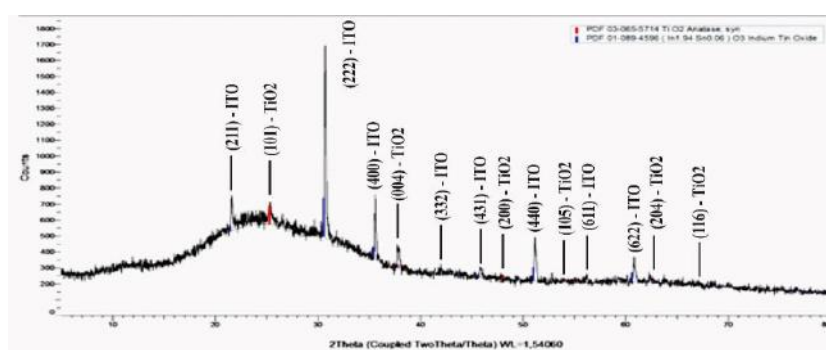


Fig. 1. XRD patterns of the Glass/ITO/TiO<sub>2</sub> structure

### 3.2. Morphological properties

The atomic forces microscopy (AFM) of the TiO<sub>2</sub> film is shown in figure 2. Nanotubes are clearly visible on the image - they are marked with arrows.

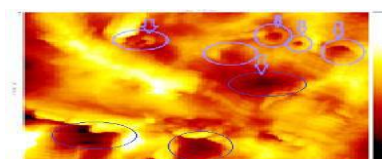


Fig. 2. AFM top view images of TiO<sub>2</sub> surface

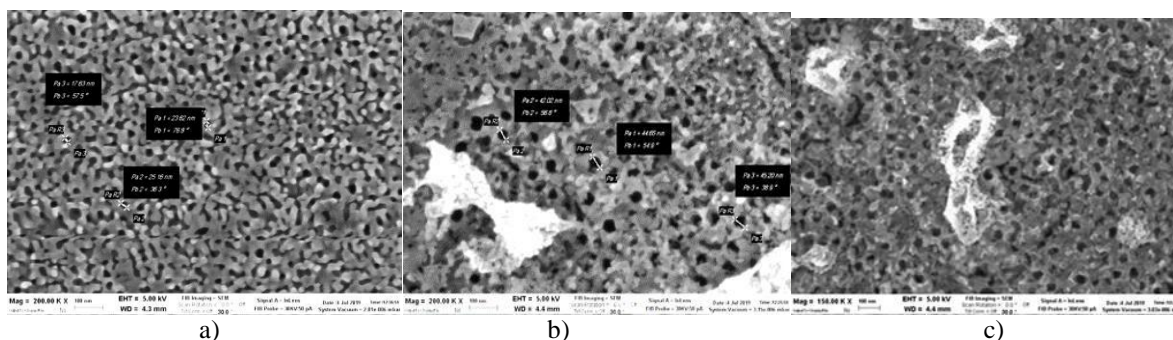


Fig. 3. SEM images of TiO<sub>2</sub> surface after different anodizing time a) 10 min.; b) 20 min.; c) 30 min

Figure 3 (a,b,c) shows SEM images of the surface of the grown films as a function of variation of the anodization time. SEM images of the samples obtained as a result of anodization for 10 minutes are given in figure 3a, whereas the images of the surface obtained as a result of anodization for 20 minutes and 30 minutes are given in figures 3b and 3c respectively.

All images show grain growth indicating crystallization, revealing that the TiO<sub>2</sub> nanotube arrays retained their nanotubular morphologies. Nevertheless, it can be seen from figure 3 that, the morphology and pore sizes of TiO<sub>2</sub> films obtained after different anodization durations are somewhat different and depend on the anodizing time. At the initial stage of anodization (10 min., figure 3a), the pores of different diameters of 17–24nm were observed only, but nanotubes are not yet visible. After 20 minutes of anodizing (figure 3b), a nanotubular structure with a diameter of about 40nm appears. After 30 min. of anodizing (figure 3c), this structure appears even more clearly. The following should also be noted: typically, RF magnetron deposited titanium thin film coating is composed of randomly oriented trapezoidal platelets on top of each other with dimensions of 100-1000nm located at some angles relative to each other [9]. The rate of anodization of these platelets varies. With short-term anodizing, part of the tile does not get enough time to be completely anodized, and additional time is required for this. As a result, a more uniform morphology is observed. Therefore, on the SEM image of the film obtained as a result of anodization for 10 and 20 min., against the background of the holes-mouths of the nanotubes, stand-alone platelets with sides of 50-100nm length are observed. The surface of the film obtained by anodizing for 30 minutes has a relatively high uniformity.

### 3.3. Raman spectroscopy

The Raman spectrum of the structure is given in figure 4. Here, arrows of black, green, and red colors are used to indicate the bands of TiO<sub>2</sub>, ITO, and glass, respectively. The observed frequencies of the Raman bands of TiO<sub>2</sub> are 143, 197, 339, 391, 513, 519, and 639cm<sup>-1</sup> and they confirm the crystalline formation of the anatase TiO<sub>2</sub> [18-20]. Indeed, the sample presented a crystalline structure, with tetragonal anatase as the major phase as follows: three 3E<sub>g</sub> nonpolar modes with frequencies 143, 197, and 639cm<sup>-1</sup>, 2B<sub>1g</sub> modes at 391 and 519cm<sup>-1</sup>, and 1A<sub>1g</sub> mode overlaps

with the B<sub>1g</sub> mode at 519cm<sup>-1</sup> [14–17] at room temperature, but they can be noticeably spectrally separated at sufficiently low temperatures.

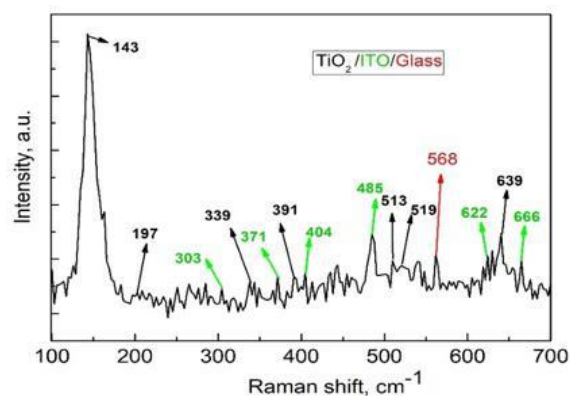


Fig. 4. Raman spectrum of the structure.

Regarding the presence of both brookite and rutile phases in the film, it should be noted that, as has been reported [15] the rutile polymorph phase may exhibit dominant peaks at 446.6 and 609.8cm<sup>-1</sup>. However, these modes of rutile haven't been observed in the Raman spectra. Further, as reported in [20], the Raman bands of anatase (399 and 639cm<sup>-1</sup>) and brookite (396 and 636 cm<sup>-1</sup>) are very close in values. Therefore, the existence of two peaks of 391 and 639cm<sup>-1</sup> observed by us initiate a question if they either refer to anatase or brookite. However, the XRD spectrum is given in figure 2, which doesn't have any peaks inherent in brookite, making it possible to completely exclude the presence of the brookite phase in the film. The bands belonging to ITO at the Raman spectrum are 303, 371, 404, 485, and 630cm<sup>-1</sup>, whereas the peak at 568cm<sup>-1</sup> are belonging to the glass substrate.

### 3.4. Optical transmission

The digital images of the samples presented in figure 5 show the change in the appearance of the Ti-coated glass/ITO structure after anodizing, as well as after subsequent thermal annealing. During the anodization process, the initially opaque Ti film (a) gradually transforms into TiO<sub>2</sub> and becomes transparent (b). Upon subsequent thermal annealing at 450°C, the optical transmission and transparency of the samples decrease as compared to non-annealed. This is because, upon annealing in the air, some additional

oxygen vacancies are introduced into the film, on which the light is scattered and the light absorption increases.

Figure 6 shows the optical transmittance of each layer of the glass substrate, *ITO* as well as  $TiO_2$  layer of the Glass/*ITO*/ $TiO_2$  bilayer structure separately. It can be seen from the spectra that the film is transparent in the region of 900–360nm with a transmittance of about 70–80% and exhibits strong absorption in the UV region with a wavelength shorter than 360nm. The latter is close to the absorption cut-off of bulk titanium dioxide and attributable to the electron's transition from valance to the conduction band of  $TiO_2$ . The wavelength region of 400–750nm showed a few interference fringes which appeared due to multiple reflections at the  $TiO_2$ /*ITO*/glass substrate and the film/air interfaces. The existence of interferometric oscillations is evident in the high optical quality of the *TNT*. A high degree of transmission allows the use of such structures to create *DSSC*.

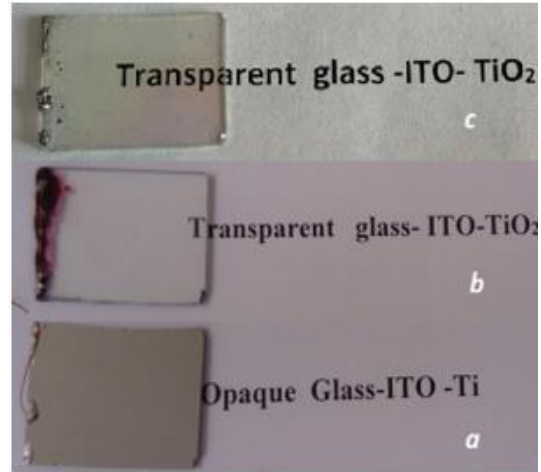


Fig.5. Optical images of the structure before a) and after oxidation (b) and upon annealing (c)

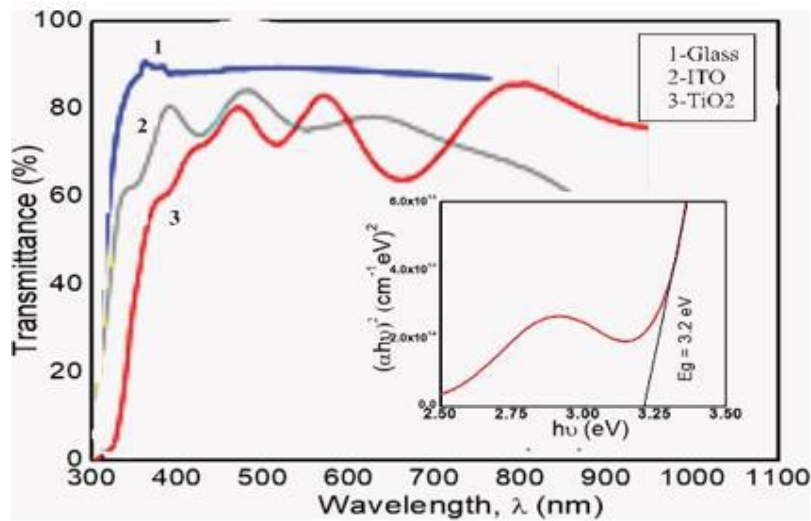


Fig.6. FTIR measurements patterns of Glass/*ITO*/ $TiO_2$  structure .1- Transmittance spectra of glass substrate, 2- *ITO*, 3-  $TiO_2$  . Inset-band gap of  $TiO_2$

Determination of bandgap energy ( $E_g$ ) is often necessary to develop the electronic band structure of a thin film material. In the high absorption region, absorption coefficient  $\alpha$  is related to the energy  $h\nu$  of incident photons by the Tauc's formula  $(\alpha h\nu) = A(h\nu - E_g)^n$ . Here  $h\nu$  is the photon energy,  $\alpha = 4\pi k/\lambda$  is the absorption coefficient at wavelength  $\lambda$ ,  $k$  –extinction coefficient,  $p$  is an index that characterizes the optical absorption process and is theoretically equal to 1/2, 2, 3/2 or 3 for direct allowed, indirect allowed, direct forbidden and indirect forbidden transitions, respectively. From the measurements and the plot of the equation, the indirect optical band gap energy,  $E_g$ , can be deduced when the linear part of the curve intercepts the x-axis just above the fundamental absorption threshold. An example of the plot of  $(\alpha h\nu)^2$  versus photon energy of the films, including extrapolation from the linear curve, is illustrated in the inset of fig. 6. From the plot, it was

determined that the  $TiO_2$  film has a direct bandgap of about 3.20eV.

### 3.3. Spectroscopic ellipsometry

Ellipsometry is a set of methods for studying the surfaces of liquid and solid bodies by changing the state of polarization of a light beam reflected by this surface and refracted on it. The relationship between the optical constants and the parameters of elliptically polarized light is established on the basis of the Fresnel equations. The ellipsometry actually measures the quantities  $\Delta$  and  $\Psi$ , which describe the change in polarization that occurs when the measurement beam interacts with a sample surface. These angles are defined by the complex ratio  $\frac{R_p}{R_s} = \tan(\psi) \exp(i\Delta)$  of Fresnel reflection coefficients for  $p$ - and  $s$ -polarized light [16-17]. The obtained data is then used to calculate the refraction index and thickness of the layer interacting with the light.



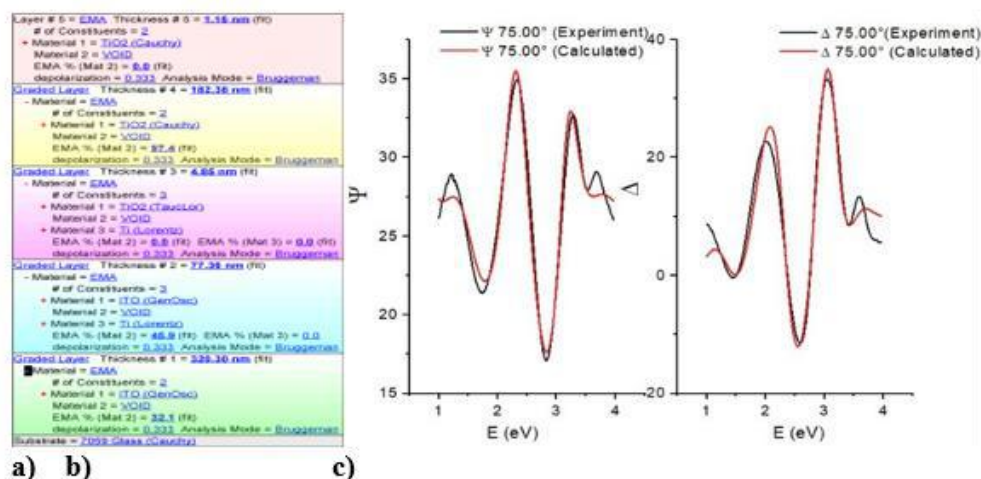


Fig.7. Schematic representation of the proposed physical model of the glass/ITO/TiO<sub>2</sub> structure (a) and illustration of generated and experimental data, curve fitting with the physical model; b) fitting on  $\psi$ , c) fitting on  $\Delta$  at incident angle 75°

The proposed physical model for SE data fitting of the annealed Glass/ITO/TiO<sub>2</sub> thin film structure is presented in Figure 7a, whereas the illustration of the calculated and experimental data, curve-fitted with the appropriated physical model is shown in Figures 6b and 6c. As it can be seen from the model, the multilayer consists of five layers with variable thicknesses and constituents. These can be listed as follows: 1) the glass substrate; 2) the 1<sup>st</sup> layer (# 320nm, consists of ITO/voids (air)-and Ti); 3) the 2<sup>nd</sup> (#77nm, ITO/VOID/Ti); 4) the 3<sup>rd</sup> (# 4.9nm, TiO<sub>2</sub>/air /Ti); 5) the 4<sup>th</sup> (#182nm, TiO<sub>2</sub> /air); 6) the 5<sup>th</sup> (# 1.15nm, TiO<sub>2</sub>/air).

#### 4. CONCLUSION

Radio-frequency magnetron sputtered titanium thin films deposited on Glass/ITO substrates have been anodized and studied. Highly ordered TNT arrays of 40-45nm pore diameter with a high degree of optical transmission were obtained. It has been established that

the surface morphology and structure of nanotubes improve with an increase in the anodization time. Ellipsometry measurements allowed to creation of an optical model of the experimentally fabricated glass/ITO/TiO<sub>2</sub> structure, consisting of five layers with different thicknesses and constituents. The XRD pattern and Raman spectra confirmed the presence of the anatase tetragonal phase of TiO<sub>2</sub> with nanotube arrays. The rutile and brookite phases were not found. By using Tauc's formula it was determined that the TiO<sub>2</sub> film has a direct bandgap of 3.20eV. It was revealed that Glass/ITO/TiO<sub>2</sub> structures are transparent in the region of 900-360nm with a transmittance of about 70– 80% and exhibit strong absorption in the UV region with a wavelength shorter than 360nm. Such a strong absorption of UV of the structure including an external TiO<sub>2</sub> layer with the extended nanotubular surface, as well as an electrically conductive ITO layer, makes it quite suitable for solar energy harvesting application

- [1] O. Durante, Di.C. Giorgio, V. Granata and et al. Emergence and Evolution of Crystallization in TiO<sub>2</sub> Thin Films: A Structural and Morphological Study. Nanomaterials., Basel., 2021., 11(6): 1409:1-18. DOI: 10.3390. nano11061409.
- [2] C. Cavallo, Di.F. Pascasio, A. Latini, M. Bonomo, D. Dini. Nanostructured Semiconductor Materials for Dye-Sensitized Solar Cells. Journal of Nanomaterials., 2017, Article ID 5323164:31. https://doi.org., 10.1155/2017/5323164.
- [3] A.A .Valeeva, E.A. Kozlova, A.S. Vokhmintsev and et al. Nonstoichiometric titanium dioxide nanotubes with enhanced catalytical activity under visible light. Sci Rep 8, 9607., 2018. https://doi.org/10.1038/s41598-018-28045-1.
- [4] P. Navabpour, K. Cooke, H. Sun. Photocatalytic properties of doped TiO<sub>2</sub> coatings deposited using reactive magnetron sputtering. Coatings. 2017,7,10. https://doi.org.,10.3390/coatings7010010.
- [5] Yen Cheng, Hui Yang, Yun Yang and et al. Progress in TiO<sub>2</sub> nanotube coatings for biomedical applications. Journal of Materials Chemistry B. 2018, 6(13):1862-1886. DOI: https://doi.org/10.1039/c8tb00149a
- [6] G. Deepak, D. Subash, G.S. Anjusree, K. Pai. Photovoltaic property of anatase TiO<sub>2</sub> 3D Meso flowers. ACS Sustainable Chem. Eng.2014; 12: pp. 2772–2780.
- [7] A. Popa, C. Ta, T. Gemming, A. Leonhardt et al. Anatase nanotubes as an electrode material for lithium-ion batteries. J. Phys. Chem. 2012;C 116: pp. 8714–8720.
- [8] D. Dumitriu, A.R. Bally, C. Ballif and et al. Photocatalytic degradation of phenol by TiO<sub>2</sub> thin films prepared by sputtering. Appl. Catal., B Environ. 2000, 25:83. DOI:10.1016/S0926-3373(99)00123-X.

- [9] *Pant Bishweshwar, Mira Park and Soo-Jin Park,\** Recent Advances in TiO<sub>2</sub> Films Prepared by Sol-Gel Methods for Photocatalytic Degradation of Organic Pollutants and Antibacterial Activities Coatings., 2019, 9(10), 613; <https://doi.org/10.3390/coatings9100613>.
- [10] *D. Rafieian, R.T. Driessen, W. Ogieglo and et al.* Intrinsic photocatalytic assessment of reactively sputtered TiO<sub>2</sub> films. ACS Appl. Mater. Interfaces. 2015: pp. 8727–8732.
- [11] *Kelly Rees,<sup>a</sup> Emanuela Lorusso,<sup>a</sup> Samuel D. Cosham,<sup>a</sup> Alexander N. Kulak<sup>b</sup> and Geoffrey Hyett.* Combining single source chemical vapour deposition precursors to explore the phase space of titanium oxynitride thin films Dalton Trans., 2018, 47, pp. 10536.
- [12] *B. Gultekin, S. Demic.* Dye-sensitized solar cells based on titanium dioxide nanoparticles synthesized by flame spray pyrolysis and hydrothermal sol-gel methods: a comparative study on photovoltaic performances. Journal of Materials Research and Technology. 2020, 9:1569-1577. DOI: 10.1016/j.jmrt.2019.11.083
- [13] *S.O. Eminov, A.S. Aliyev, J.A. Guliyev et al.* Photo and electrical peculiarities of the nanostructured glass/ITO/AAO and glass/ITO/CdS systems. Journal of Materials Science: Materials in Electronics; 2016, 27: 9853-9860. <https://DOI.org/10.1007/s10854-016-5053-9>
- [14] *A. Sadek, H. Zheng, K. Latham, et.al.* Anodization of Ti thin film deposited on ITO. Langmuir. 2009, 25: 509-514. DOI:10.1021/la802456r
- [15] *T. Stergiopoulos, A. Valota, V. Likodimos et al.* Dye-sensitization of self-assembled titania nanotubes prepared by galvanostatic anodization of Ti sputtered on conductive glass. Nanotechnology, 2009, 20(31):365601. DOI: <https://doi.org/10.1088/0957-4484/20/36/365601>.
- [16] *M. Horprathum, P. Chindaudom.* A Spectroscopic ellipsometry study of TiO<sub>2</sub> thin films prepared by dc reactive magnetron sputtering: annealing temperature effect. Chinese Physics Letters. 2007;24(6):1505. DOI: <https://doi.org/10.1088/0256-307X/24/6/021>.
- [17] *J.A. Woollam, B. Johs, Herzinger Craig M. et al.* Overview of variable angle spectroscopic ellipsometry (VASE), Part I: Basic theory and typical applications Proc. SPIE 10294, Optical Metrology: A Critical Review, 1999, 1029402. DOI: 10.1117/12.351660.
- [18] *E.J. Ekoi, A. Gowen, R. Dorrepaal, D.P. Dowling.* Characterization of titanium oxide layers using Raman spectroscopy and optical profilometry: Influence of oxide properties. Results in Physics, 2019;12:1574-1585. <https://doi.org/10.1016/j.rinp.2019.01.054>.
- [19] *E.J. Ekoi, C. Stallard, I. Reid, D.P. Dowling.* Tailoring oxide-layer formation on titanium substrates using microwave plasma treatments. Surf Coat Technol. 2017, 325. <https://doi.org/10.1016/j.surfcoat.2017.06.046>.
- [20] *F.D. Hardcastle.* Raman spectroscopy of titania (TiO<sub>2</sub>) nanotubular water-splitting catalysts. J. Ark. Acad. Sci. 2011, 65: pp. 43–48.